Research Article/Araştırma Makalesi

GAZİ
JOURNAL OF ENGINEERING SCIENCES

The Effect of Fe Addition on High-Temperature Transformations of Specific Silica Sources

Cengiz Bagci[a,*], Murat Zengin[b], Burak Kaya[c], Ozgür Güven[d]

Submitted: 07.02.2023 Revised: 19.04.2023 Accepted: 16.06.2023 doi:10.30855/gmbd.0705072

ABSTRACT

Alternative sources of silica, most abundant in the earth's crust, are converted into useful high-temperature crystalline phases. In this study, temperature dependent phase transformations of silica sand and rice husk sourced silica with and without the addition of 10 % by weight elemental iron were investigated. For this purpose, firstly, the initial silica sources were calcined at 700 °C for 2 hours, ground into fine powder and placed on a carbon substrate and heat treated in a tube furnace at 1500 °C for 2 hours in argon atmosphere. The phase transformation characteristics of the final material were made by XRD and SEM analysis. A mixture of cristobalite-tridymite and high purity cristobalite was observed in rice husk ash with and without Fe addition, respectively. In the same order, XRD phase pure tridymite and cristobalite phases were observed in silica sand. As a result, XRD phase pure or tailored transformations of these crystalline phases were obtained depending on the Fe addition and silica source.

Keywords: Silica sand, rice husk, cristobalite, tridymite

[a,*] Hitit University, Faculty of Engineering, Dept. of Metallurgical and Materials Engineering, 19030-Corum, Türkiye Orcid: 0000-0001-9931-0778 e mail: cengizbagci@gmail.com

[b] Hitit University, Faculty of Engineering, Dept. of Metallurgical and Materials Engineering, 19030-Corum, Türkiye Orcid: 0000-0002-3980-1062

[c] Hitit University, Faculty of Engineering, Dept. of Metallurgical and Materials Engineering, 19030-Corum, Türkiye Orcid: 0000-0002-6218-7021

[d] Hitit University, Faculty of Engineering, Dept. of Metallurgical and Materials Engineering, 19030-Corum, Türkiye Orcid: 0000-0002-2969-2085

*Corresponding author: cengizbagci@gmail.com

Belirli Silika Kaynaklarının Yüksek-Sıcaklık Dönüşümlerinde Fe İlavesinin Etkisi

ÖZ

Alternatif silika kaynakları yer kabuğunda bol bulunduklarından, yararlı yüksek sıcaklıkta kristal fazlara dönüştürülürler. Bu çalışmada, ağırlıkça % 10 elemental demir katkılı ve katkısız silis kumu ve pirinç kabuğu esaslı silislerin sıcaklığa bağlı faz dönüşümleri incelenmiştir. Bu amaçla, ilk olarak başlangıç silika kaynakları 700 °C' de 2 saat kalsine edilmiş, ince toz haline getirilmiş ve bir karbon altlık üzerine yerleştirildikten sonra argon atmosferinde 1500 °C'de bir tüp fırında 2 saat ısıl işleme tabi tutulmuştur. Nihai malzemenin faz dönüşüm karakteristikleri XRD ve SEM analizi ile yapılmıştır. Fe katkılı ve katkısız pirinç kabuğu külünde sırasıyla bir kristobalit-tridimit karışımı ve yüksek saflıkta kristobalit gözlenmistir. Aynı sıra ile silis kumunda XRD faz saf tridimit ve kristobalit fazları gözlenmiştir. Sonuç olarak, Fe katkisina ve silis kaynağına bağlı olarak bu kristal fazların XRD faz saf veya uyarlanmış dönüşümleri elde edilmistir.

Anahtar Kelimeler: Silika kumu, pirinç kabuğu, kristobalit, tridimit

To cite this article: C. Bagci, M. Zengin, B. Kaya, and O. Guven, "The Effect of Fe Addition on High-Temperature Tranformations of Specific Silica Sources," *Gazi Journal of Engineering Sciences,* vol. 9, no. 2, pp. 304-309, 2023. doi:10.30855/gmbd.0705072

1. Introduction

Following oxygen, silicon is the most abundant element in the earth's crust and together they form silica. Containing a minimum 98 % SiO_2, silica sand is a hard mineral that is very resistant to temperature and chemical effects [1]. Because of these intrinsic properties, it is always used in different industries, for example, on the floors where heavy equipment is working, where high abrasion resistance is required, it is used safely in construction and in the production of building chemical materials due to its structure that is not affected by acids [2]. Rice is one of the most important food sources in the world, 72 % of which is consumed by humans and then the husk remains as natural waste. Rice husk contains silica (70-90 %) depending on the geography and climatic conditions where the rice is grown. The type and amount of silica in the husk depend on the calcination temperature and time. Rice husk ash is obtained by burning rice husk at temperatures over 500 °C and contains a little carbon of organic origins. It is used as a source of silica in the production of geopolymer [3], concrete or high-temperature composites and ceramics such as SiC [4], Si_3N_4 [5]. Silica is a polymorph material that can change its molecular structure with temperature. Silica, which is in the form of crystalline quartz at low temperatures, transforms into the crystalline tridymite phase at 870 °C and forms cristobalite at around 1470 °C [6-8]. These refractories can be effectively utilized in various areas such as glass, paints, ceramics, plastics, and construction products [9, 10].

In terms of contributing to the circular economy with a sustainable and waste-reducing approach, these two silica resources can be effectively used in the transformation of these useful refractories. There is limited study in literature directly related to the current study; however, the addition of iron was reported as 3-17 wt. % in a related study [11]. 10 % wt. iron addition was fixed, considering that the low amount of iron would act as a trace metal and the excess amount of iron would promote single-phase cristobalite conversation [12, 13]. In this study, temperature-dependent phase transformations of silica sand and rice husk-sourced silica with and without the addition of 10 % by weight elemental iron were investigated.

2. Materials and Methods

Silica sand and rice husk used as local silica sources in this study were obtained from Samsun and Osmancık, respectively. Elemental Fe was used as the catalyst and graphite plate was used as the substrate. First, both silica sources were calcined at 700 °C for 2 hours in an open-air furnace to remove possible organic compounds. Following the calcination, they were ground into powders in a mortar and pestle and subsequently sieved to 63 µm particle sizes. With their use without additives, the initial samples were homogenized in a planetary ball mill (Fritsch Pulverisette 7) with YSZ (ZrO_2 and Y_2O_3) vessel and balls by adding elemental Fe 10 % to both silica sources. The designed samples are based on silica sand (SS) and rice husk ash (RHA) deemed as SS-0, SS-10, RHA-0, and RHA-10. Simultaneously, surface cleaning processes of graphite substrates were carried out in Daihan Wish WUC-D22H brand ultrasonic bath device. The heat treatment of the samples was carried out in the PTF 16/75/450 model atmosphere-controlled tube furnace. 0.5 grams of powder was taken from each sample and placed on the graphite substrate in such a way that they do not come into contact with each other, and then the substrate was inserted in the center of the furnace where the temperature changes were the least, and the lids of the tube were closed (Fig. 1a). The heat treatments were carried out by providing a continuous flow of argon gas from the tube within the program including two isothermal soaks at 750 °C and 1500 °C for 0.5 and 2 h in Fig. 1b, respectively.

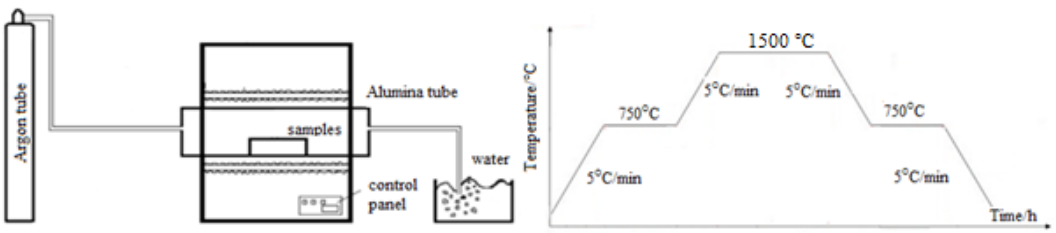

Figure 1. Tube furnace set-up and heat-treatment program.

Following the reaction products were ground into a fine powder, and the EMPYREAN diffractometer (λ = 0.15418 nm, mean of λ1 and λ2) equipped with a CuKα source was analyzed by PANanalytical X-ray diffraction. The tests used a voltage of 40 kV, a current of 30 mA, a rise of 0.02, (2θ), a Bragg angle from 10° to 80° (2θ), and a scan rate of 1°/min. The resulting peaks were defined manually by matching with single Jade

9 software. Microstructure images of the synthesized powders (Quanta 450 SEM) were obtained by scanning electron microscope at 25K magnification, 10-20 kV voltage range, and high vacuum and with a secondary electron detector. Crystallite sizes of transformed phases calculated considering the XRD peak of every converted phase by the Debby scherer equation $D=0.9\ \lambda/(\beta_{1/2}\cos\theta)$, where λ=X-Ray wavelength, $\beta_{1/2}$=calculated with half-maximum of the strongest peak, θ=diffraction angle and d= crystallite size.

3. Results and Discussion

Fig. 2 shows the XRD pattern of all the samples heat treated in a tube furnace at 1500 °C for 2 hours in a flowing argon atmosphere. Morphological and chemical content characterizations of the rice husk used in this study by SEM-EDS before and after calcination were reported in our most recent study [4]. In EDS analysis, while silicon and oxygen constitute the majority of the chemical content by weight percent, 5 % potassium and carbon were found as the most following content and the rest consists of trace elements. It has also been evaluated in other studies that surface oxides formed during calcination cause carbon that has not been removed from the rice husk ash [14]. However, it is seen that the unburned carbon in the final product is completely removed from the structure upon heating at 1500 °C for 2 hours after calcination in the current study. A mixture of both cristobalite and tridymite polymorphs is seen in sample RHA-10. Here, it is concluded that iron inhibits cristobalite formation in a limited way. Fibrous rice husk was able to ground into a finer grain size than silica sand, which has a Mohs hardness of around 7 after calcination with pestle and mortar.

Therefore, the high surface area of rice husk allowed a high iron-derived liquid phase on the surface of the grains, partially preventing cristobalite formation. In the rice husk sample without iron addition, RHA-0, severe XRD phase pure cristobalite peaks were observed. Tridymite nearly transforms into cristobalite at 1470 °C with polymorphic transformation seen between (25-30°)=2-theta in the RHA-0 sample [15].

XRD phase pure tridymite formation with a total of four main characteristic peaks, three between 20°-30° 2-theta and one with 36° 2-theta is observed as a result of XRD performed after heat treatment of SS-10 sample [16]. In the case of SS-0 without iron addition, cristobalite formation, which is a high-temperature polymorph of silica, shifts the tridymite peaks to cristobalite. This can be explained by the fact that the addition of iron in the SS-10 sample forms a eutectic phase due to high-temperature heat treatment and predominantly prevented the formation of cristobalite. In addition to the cristobalite form of silica, some graphite peaks originating from the graphite substrate are also observed in the SS-0 sample. The structural integrity of the graphite substrate is disrupted by high temperatures, and efflorescence occurs on its surface that can easily diffuse to the samples on it. These degradations were easily seen from the naked eye inspection of the graphite substrate after the experiment.

Since iron differently inhibited cristobalite formation in both silica sources, this resulted in the formation of mixed structures of cristobalite and tridymite in different amounts. Depending on the desired properties of the resulting material, the starting composition and heat treatment can be designed.

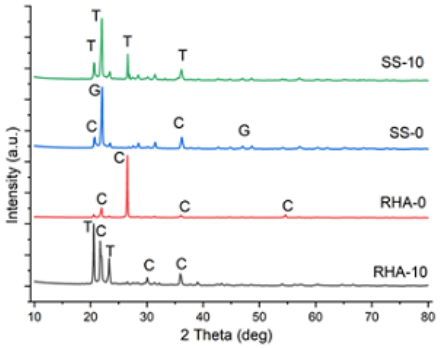

Figure. 2. XRD patterns of SS-0, SS-10, RHA-0, RHA-10 samples heat treated in a tube furnace at 1500 °C for 2 hours in argon atmosphere. C: Cristobalite, T:Tridymite, G:Graphite).

The SEM micrographs of RHA-0 and RHA-10 samples heat treated in a tube furnace at 1500 °C for 2 hours in an argon atmosphere are shown in Fig 3. The general microstructure in Fig 3a is mainly composed of

hexagonal particles ascribed to typical tridymite formation consistent with XRD (a crystallite size 3.62 at 2 theta=20.57) results in Fig. 2 [17]. On the other hand, with the effect of 10 percent iron addition, some of the hexagonal particles grew into fibers having 10 µm in width and about two micrometers in length (Fig 3b) [13, 19]. The formation mechanism of SiO_2 fibers could be expressed by the following reaction;

$$2CO_{2\,(g)} + Si_{(s)} \longrightarrow 2CO + SiO_2 \qquad (1)$$

Fiber formation with high a aspect ratio depends on a catalyst-assisted vapor-liquid-solid mechanism [20]. In the current study iron promoted to increase the fiber formation by playing as a catalyst. Fig 3c reveals a homogeneous tailored morphology of traditional hexagonal prismatic, leaf-like and lath-shaped of cristobalite with a crystallite size of 4.63 at 2 theta=26.53. The hexagonal grains are approximately 20 µm in size and there are leaf-like and lath-shaped particles of 1-2 µm both sizes, which are relatively regularly distributed in the main hexagonal structure [21]. The shapely tailored morphology can contribute to the strength of the ceramic materials to be produced from these powders by creating a driving force for sintering due to the structural difference, both in this way and in terms of increasing the fracture toughness of the lath-shaped parts in the structure [22].

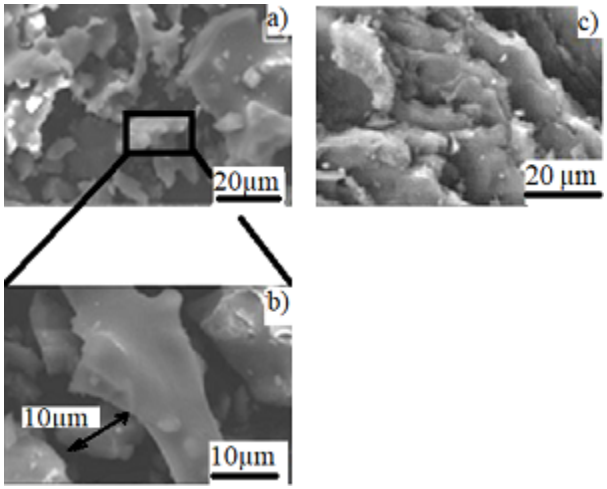

Figure 3. (a) General SEM micrographs **of** RHA-10, b) high magnification image of fibrous, (c) RHA-0 samples heat treated in a tube furnace at 1500 °C for 2 hours in an argon atmosphere**.**

Fig. 4 depicts the SEM micrographs of SS-0 and SS-10 samples heat treated in a tube furnace at 1500 °C for 2 hours in an argon atmosphere**.** By the evaluation made in the XRD analysis (Fig.2), it is seen that the microstructure consists of coarser crystals when compared to the powders synthesized from rice husk in the general image the Fig 4a. From the magnified image in Fig. 4b, it is deduced that the grains are about 100 microns and about 10 times larger than the sizes of the powders synthesized from this rice husk [23]. Similar to powders synthesized from rice husk, hexagonal and fiber-shaped bimodal morphology is observed. This is consistent with the detection of tridymite-cristobalite with a crystallite size of 2.56 at 2 theta=21.97 in XRD analyses. The addition of iron could not complete the tridymite-cristobalite transformation due to its coarse structure, and this allowed mixing the structure as a phase as well as shape tailoring [24]. Long enough fibers with a width of 20 µm in the structure can be effective in the crack deflection mechanism in the ceramic material to be produced from these powders [25]. A more uniform structure consisting of coarse agglomerated and fine spherical-shaped particles is seen in Fig. 4c and this structure is adjusted to phase pure cristobalite as seen from the XRD analysis with a crystallite size 2.81 at 2 theta=22.03.

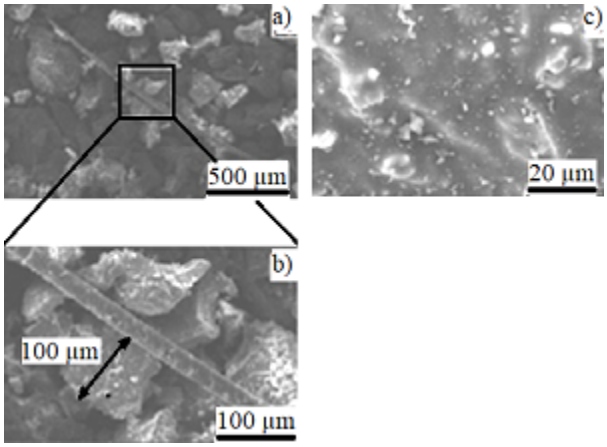

Fig.ure 4. (a) General SEM micrographs **of** SS-10, b) high magnification image of fibrous, (c) SS-0 samples heat treated in a tube furnace at 1500 °C for 2 hours in an argon atmosphere**.**

4. Conclusion

As a result, it was observed that the addition of elemental iron had different effects on the high-temperature transformations of silica sand and rice husk ash. While the Fe-added silica sand sample resulted in phase pure tridymite, the non-added silica sand ash resulted in a mixture of cristobalite and graphite. On the other hand, the tridymite-cristobalite binary structure was obtained from the iron-added rice husk ash, while phase pure cristobalite was obtained from the non-added. While iron provides phase pure tridymite transformation in rice husk ash due to its fine grain size, a binary structure is achieved in coarse-grained silica sand due to the incomplete tridymite-cristobalite transformation. The presence of phase in the resulting material can be controlled by adding iron to the initial silica sources. In addition to its environmentally friendly approach to waste reduction, the tailored refractories synthesized in this study are proposable for various industries such as glass, paints, ceramics, plastics, and construction products.

Acknowledgment

The study was carried out in the laboratories of the Department of Metallurgical and Materials at Hitit University.

Conflict of Interest Statement

The authors declare that there is no conflict of interest

References

[1] R. Ratnawulan, A. Fauzi and A. E. S. Hayati, "Characterization of silica sand due to the influence of calcination temperature," *IOP Conference Series: Materials Science and Engineering*, vol. 335 no. 1, pp. 012008, 2018. **doi:**10.1088/1757-899X/335/1/012008.

[2] N. Soltani, A. Bahrami, M. I. Pech-Canul and L. A. González, "Review on the physicochemical treatments of rice husk for production of advanced materials," *Chemical Engineering Journal*, vol. 264, pp. 899-935, 2015. doi:10.1016/j.cej.2014.11.056

[3] U. H. Heo, K. Sankar, W. M. Kriven and S. S. Musil, "Rice husk ash as a silica source in geopolymer formulation," *Ceramic Engineering and Science Proceedings,* vol. 38, no. 10, pp. 87-102, 2015. doi:10.1002/9781119040293.ch7

[4] C. Bagci, K. Karacif, B. Alkan and H. Arik, "The use of rice husk ash-based SiC particles as reinforcement in geopolymer composites," *Journal of Polytechnic*, (early view), 2023. doi:10.2339/politeknik.1130886

[5] S. S. Hossain, L. Mathur and P. K. Roy, "Rice husk/rice husk ash as an alternative source of silica in ceramics: A review," *Journal of Asian Ceramic Societies*, vol. 6, no. 4, pp. 299-313, 2018. doi:10.1080/21870764.2018.1539210

[6] P. J. Heaney, "Structure and chemistry of the low-pressure silica polymorphs", silica physical behaviour," *Geochemistry and Materials Applications*, vol. 29, pp. 1-32, 1994. doi:10.1515/9781501509698-006

[7] T. Demuth, Y. Jeanvoine, J. Hafner and J. G. Angyan, "Polymorphism in silica studied in the local density and generalized-gradient approximations," *J. Phys.: Condens. Matter*, vol.11, pp 3833–3874,1999. doi:10.1088/0953-8984/11/19/306

[8] K. Mohanta and P. Bhargava, "Effect of milling time on the rheology of highly loaded aqueous-fused silica slurry," *J. Am. Ceram. Soc.*, vol. 91, no. 2, pp 640–643, 2008. doi:10.1111/j.1551-2916.2007.02153.x

[9] X. Yang, D. Lu, B. Zhu, Z. Sun, G. Li, J. Li, Q. Liu and G. Jiang, "Phase transformation of silica particles in coal and biomass combustion processes," *Environmental Pollution*, vol. 292, pp. 118312, 2022. doi:10.1016/j.envpol.2021.118312

[10] M. J. Kaleli, P. K. Kamweru, J. M. Gichumbi and F. G. Ndiritu, "Characterization of rice husk ash prepared by open air burning and furnace calcination," *Journal of Chemical Engineering and Materials Science*, vol. 11, no. 2, pp. 24-30, 2020. doi:10.5897/JCEMS2020.0348

[11] K. N. Maamur, U. S. Jais, and S. Y. S. Yahya, "Magnetic phase development of iron oxide-SiO_2 aerogel and xerogel prepared using rice husk ash as precursor," In AIP Conference Proceedings, vol. 1217, no. 1, pp. 294-301, 2010,. doi:org/10.1063/1.3377832

[12] N. P. Hoolikantimath, K. G. Guptha, R. K. Rao and P. A. Ghorpade, "Effect of temperature on sodium silicate bonded sand and its phase transformations to cristobalite in metal casting industry," *JOM*, vol. 74, no. 2, pp. 465-473, 2022. doi:10.1007/s11837-021-05056-4

[13] N. P. Hoolikantimath, S. Dodamani, K. G. Guptha, R. K. Rao and P. A. Ghorpade, "Influence of metal casting temperature and cations on phase transformation of silica sand to cristobalite," *International Journal of Metalcasting*, pp. 1-12. 2022. doi:1007/s40962-022-00921-7

[14] S. A. Saad, A. N. Jamaluddin, S. A. Masjuki, S., Beddu and N. Shafiq, "Influences of grinding process on the physical and morphological characteristics of ultrafine treated rice husk ash," *Geomate Journal*, vol. 23, no. 97, pp. 74-81, 2022. doi:10.21660/2022.97.3117

[15] Y. Shinohara and N. Kohyama "Quantitative analysis of tridymite and cristobalite crystallized in rice husk ash by heating," *Industrial health*, vol. *42*, no. 2, pp. 277-285, 2004. doi:10.2486/indhealth.42.277

[16] U. Nurbaiti and S. Pratapa, "Synthesis of cristobalite from silica sands of Tuban and Tanah Laut," *In Journal of Physics: Conference Series*, vol. 983, no. 1, pp. 012014, 2018. doi:10.1088/1742-6596/983/1/012014

[17] R. D. Febo, L. Casas, Á. A. del Campo, J. Rius, O. Vallcorba, J. C. Melgarejo and C. Capelli, "Recognizing and understanding silica-polymorph microcrystals in ceramic glazes," *Journal of the European Ceramic Society*, vol. 40, no. 15, pp. 6188-6199, 2020. doi:10.1016/j.jeurceramsoc.2020.05.063

[18] A. T. Vu, T. N. Xuan and C. H. Lee, "Preparation of mesoporous Fe_2O_3·SiO_2 composite from rice husk as an efficient heterogeneous Fenton-like catalyst for degradation of organic dyes," *Journal of Water Process Engineering*, vol. 28, pp.169-180, 2019. doi:10.1016/J.JWPE.2019.01.019

[19] V. Erofeev, A. Yusupova and A. Bobrishev, "Activation of sulfur and opal-cristobalite-tridymite phase in sulfur concrete technology," *IOP Conference Series: Materials Science and Engineering*, vol. 463, no. 4, pp. 042033, 2018. doi:10.1088/1757-899X/463/4/042033

[20] S. Pukird, P. Chamninok, S. Samran, P. Kasian, K. Noipa and L. Chow, "Synthesis and characterization of SiO_2 nanowires prepared from rice husk ash," *Journal of Metals, Materials and Minerals*, vol. 19, no. 2, pp. 33-37, 2009.

[21] A. Gupta, V. Pandey, M. K. Yadav, K. Mohanta and M. R. Majhi, "A comparative study on physio-mechanical properties of silica compacts fabricated using rice husk ash derived amorphous and crystalline silica," *Ceramics International*, vol. 48, no. 23, pp. 35750-35758, 2022. doi:10.1016/j.ceramint.2022.07.098

[22] F. Z. Sobrosa, N. P. Stochero, E. Marangon and M. D. Tier, "Development of refractory ceramics from residual silica derived from rice husk ash," *Ceramics International*, vol. 43, no. 9, pp. 7142-7146, 2017. doi:10.1016/j.ceramint.2017.02.147

[23] Zainuri, M. "Synthesis of SiO nanopowders containing quartz and cristobalite phases from silica sands," *Materials Science-Poland*, vol. 33, no. 1, pp. 47-55, 2015. doi:10.1515/msp-2015-0008

[24] S. Kwon, Y. Kim and Y. Roh, "Effective cesium removal from Cs-containing water using chemically activated opaline mudstone mainly composed of opal-cristobalite/tridymite (opal-CT)," *Scientific Reports*, vol. 11, no. 1, pp. 1-15, 2021. doi:10.1038/s41598-021-94832-y

[25] X. H. Zhang, Y. Li, Z. H. Tian, Y. Sun, C. H. Ma and Q. Y. Zheng, "Transformation mechanisms of cemented silica and crystalline silica to tridymite in silica bricks," *Interceram-International Ceramic Review*, vol. 71, no. 3, pp. 20-29, 2022. doi:10.1007/s42411-022-0505-0